Conversion of evanescent waves into propagating waves by vibrating knife edge

S. Samson, A. Korpel and H.S. Snyder

Department of Electrical and Computer Engineering, 4400 Engineering Bldg., The University of Iowa, Iowa City, IA 52242.

Abstract

Using plane wave spectrum methods, we analyze the propagation and mutual conversion of plane and evanescent waves generated by a one-dimensional object partially obscured by a vibrating knife-edge. We show that sub-wavelength details of the object may be detected in each part of the transmitted plane wave spectrum, upon scanning the knife edge across the object. We discuss the implications for near-field scanning optical microscopy (NSOM) and compare some aspects of conventional NSOM (physical aperture), and vibrating knife edge (electronic aperture) approaches to the sampling of optical fields.

Key Words: plane wave spectrum, near-field scanning optical microscopy (NSOM), vibrating knife edge.

I. Introduction

In previous papers [1-4] we have discussed the one- and two-dimensional operation of an optical microscope that uses a vibrating knife edge. In these papers, the analysis is simplified by assuming that *all* light power passing both the specimen and an opaque knife edge is detectable. In practical situations this is not realizable, since evanescent waves do not propagate away from the specimen, and therefore are not directly detectable.

High spatial frequency details (spatial frequencies greater than $1/\lambda$, for light that is incident perpendicular to the subject) in the specimen cause evanescent waves to be created. Because this information does not propagate through free space, small spatial details cannot be imaged by conventional microscopes, where the image is formed by propagating the light through a series of lenses. For this reason conventional microscopes cannot increase their resolution much past a spatial frequency of $1/\lambda$. (The absolute limit is $2/\lambda$ for grazing incident illumination.)

In the last decade, several schemes for detecting evanescent waves were introduced [5, 6, 7]. They all use a sub-wavelength-sized pinhole aperture that samples the field very close (less than λ) to the specimen. By positioning the aperture in this manner, the evanescent waves are converted into propagating waves, which may then be detected. The aperture is raster-scanned across the specimen surface to create a two-dimensional image of the specimen on a computer.

In our technique, we use a vibrating knife-edge or knife edge corner to scatter and/or convert the field perturbed by the specimen, after which it is collected by conventional lenses. In this paper we calculate the power in the collected light, and analyze in detail how spatial information is retrieved from the scattered and converted waves. This is done using plane wave spectrum methods [8,9].

Our paper is organized as follows: in section 2, the propagation of waves scattered by an object is analyzed, with and without a knife edge inserted. In section 3, the results of section 2 are analyzed using graphical methods. In section 4, we compare some aspects of the pinhole aperture and vibrating knife edge method of sampling evanescent fields. In section 5, we state conclusions and propose future research.

II. Theory

The subsequent analysis is limited to the one-dimensional case for simplicity. Time-dependence will be assumed to be $\exp(j\omega t)$, so that a +Z propagating plane wave of monochromatic light is written in phasor notation as $E_o \exp(-jkz)$, where $k=2\pi/\lambda$.

A. Evanescent wave generation by an object

The configuration to be analyzed is as follows. Plane waves of light, propagating in the +Z-direction are incident on an amplitude grating t(x) at z=0. The (phasor) field before the grating will be defined for convenience as a real constant

$$E^{-}(x,0) = E_o\, e^{-jk0} = E_o \tag{1}$$

The amplitude transmittance of the (constant phase) amplitude grating is chosen as

$$t(x) = 1 + m\cos(K_x x) \tag{2}$$

where m is the amplitude modulation index of the grating and K_x the wavenumber of the grating (= $2\pi/\Lambda$, Λ is the grating period). A sinusoidal grating is chosen since an arbitrary object may be Fourier-decomposed into a summation of sine and cosine gratings. In a realizable grating t(x) < 1, but we ignore this aspect here for notational convenience.

The field after the grating, at $z=0^+$, is given by

$$E_o^{+}(x) = E_o[1+ m\cos(K_x x)] \tag{3}$$

The (1-dimensional) plane wave spectrum of the field at $z=0^+$ is calculated as the inverse Fourier transform of $E_o^{+}(x)$ [8]:

$$A_o^{+}(k_x) = \int_{-\infty}^{+\infty} \{E_o^{+}(x)\}\exp(jk_x x)\,dx \tag{4a}$$

$$= E_o\left[\,\delta(k_x) + \frac{m}{2}\delta(k_x - K_x) + \frac{m}{2}\delta(k_x + K_x)\right] \tag{4b}$$

which represents the sum of three plane waves, propagating in different directions.

Now, the wave propagator for free space, which describes how the plane waves are propagated, [9] is given as

$$H_z = \exp(-jk_z z) \tag{5}$$

where $k_z^2 = k^2 - k_x^2 - k_y^2$. For our case ($k_y = 0$), we substitute $k_z = k\sqrt{1 - k_x^2}$ to obtain

$$H_z = \exp\left(-jz\sqrt{k^2 - k_x^2}\right) \tag{6}$$

Which results in the plane wave spectrum at the plane z

$$A_z(k_x) = E_o[\,\delta(k_x) + \frac{m}{2}\delta(k_x - K_x) + \frac{m}{2}\delta(k_x + K_x)] \times \exp(-jz\sqrt{k^2 - k_x^2}) \tag{7}$$

Taking the Fourier transform of eq. (7) yields the electric field at z:

$$\begin{aligned} E_z(x,z) &= \int_{-\infty}^{\infty} A_z(k_x)\exp(-jk_x x)\,dk_x \\ &= E_o \exp(-jkz) \\ &+ E_o \frac{m}{2}\exp(-jz\sqrt{k^2 - K^2})\exp(-jKx) \\ &+ E_o \frac{m}{2}\exp(-jz\sqrt{k^2 - K^2})\exp(+jKx) \end{aligned} \tag{8}$$

It will be seen that for the case of $\Lambda < \lambda$, the second and third terms of eq.(8) are evanescent waves propagating in the ±x directions with wavenumber K_x, and decaying exponentially in amplitude in the z-direction (the $\exp(-jz\sqrt{k^2 - K^2})$ terms become real). Traditional microscopes cannot see details smaller than the wavelength of light because they cannot detect these evanescent, non-propagating waves.

B. Evanescent-to-plane wave conversion by the knife edge

We now place a knife edge in the plane of the object (z=0) at $x=x_o$. The simple assumption is made that the knife edge geometrically obscures the incoming plane waves of light for $x \le x_o$ and transmits for $x > x_o$. We will show that, by varying the position of the knife edge in the x-direction, spatial information about the grating may be ascertained, even if the grating period is sub-wavelength. To avoid infinite power problems in the calculations and more closely model actual practice, the beam size at the grating is limited to a width L in the x-direction, and its amplitude is assumed to be constant from $-L/2 \le x \le L/2$.

As illustrated in Fig. 1, the amplitude grating transmittance of eq. (2), with the input beam limits included becomes

$$t(x') = 1 + m\cos[K_x (x'+d)] \quad \text{if } -a \le x' \le a$$
$$= 0 \quad \text{otherwise} \tag{9}$$

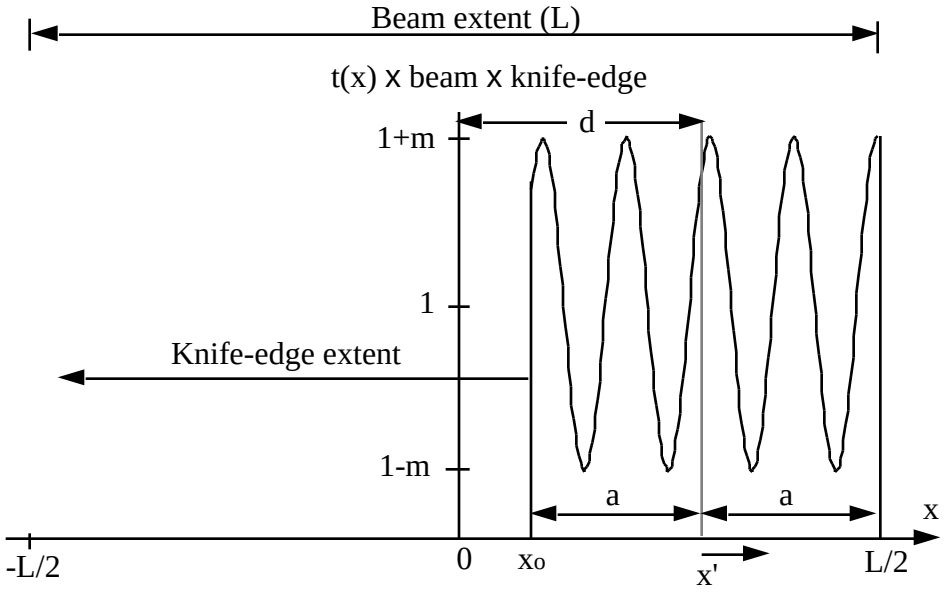

Figure 1. Knife-edge limited sinusoidal amplitude grating

where, for mathematical convenience, we have introduced the variables

$$a = \frac{L}{4} - \frac{x_0}{2}$$
$$d = \frac{x_0}{2} + \frac{L}{4} \quad \text{and}$$
$$x' = x - \frac{x_0+L/2}{2} = x - d \tag{10}$$

We wish to calculate the plane wave spectrum of the knife-edge truncated field and analyze how this depends on the knife edge position and the grating parameters. The plane wave spectrum is proportional to the Fraunhofer diffraction pattern, or the field seen at the back focal

plane of a lens, with the grating/knife edge at the front focal plane. Because the propagating plane waves will be detected by a photodetector, which converts *intensity* (power) into electrical signals, the final results will be given in intensities.

The plane wave spectrum of the field at $z=0^+$ is given by

$$A(k_{x'}) = \int_{-a}^{a} E_o\,(1+m\cos[K_x\,(x'+d)])\exp(jk_{x'}x')\,dx' \qquad (11)$$

Eq. (11) is readily evaluated:

$$A(k_{x'}) = E_o a \left\{ 2\,\frac{\sin(k_{x'}a)}{k_{x'}a} + m\exp(jK_x d)\,\frac{\sin[(K_x + k_{x'})a]}{(K_x + k_{x'})a} + m\exp(-jK_x d)\,\frac{\sin[(K_x - k_{x'})a]}{(K_x - k_{x'})a} \right\} \qquad (12)$$

This may be interpreted as three delta functions in the plane wave spectrum, centered at $k_{x'} = 0$, $+K_x$ and $-K_x$, and convolved with $\sin(k_{x'}a)/k_{x'}a = \mathrm{sinc}(k_{x'}a/\pi)$. To visualize eq. (12), it was entered into the mathematical analysis package *Maple V* on a Macintosh II computer. This program allows the user to plot an equation as a function of one or two variables. The amplitude of the plane wave spectrum, for the case of $K_x = 2\pi/\Lambda = 0.5\text{x}10^6$ and m = 0.5, $a=10\Lambda$, $d=n(2\pi/K_x)$ (n is an integer) is shown in figure 2.

The relative *intensity* of light in the plane wave spectrum, is found by multiplying eq.(12) with its complex conjugate:

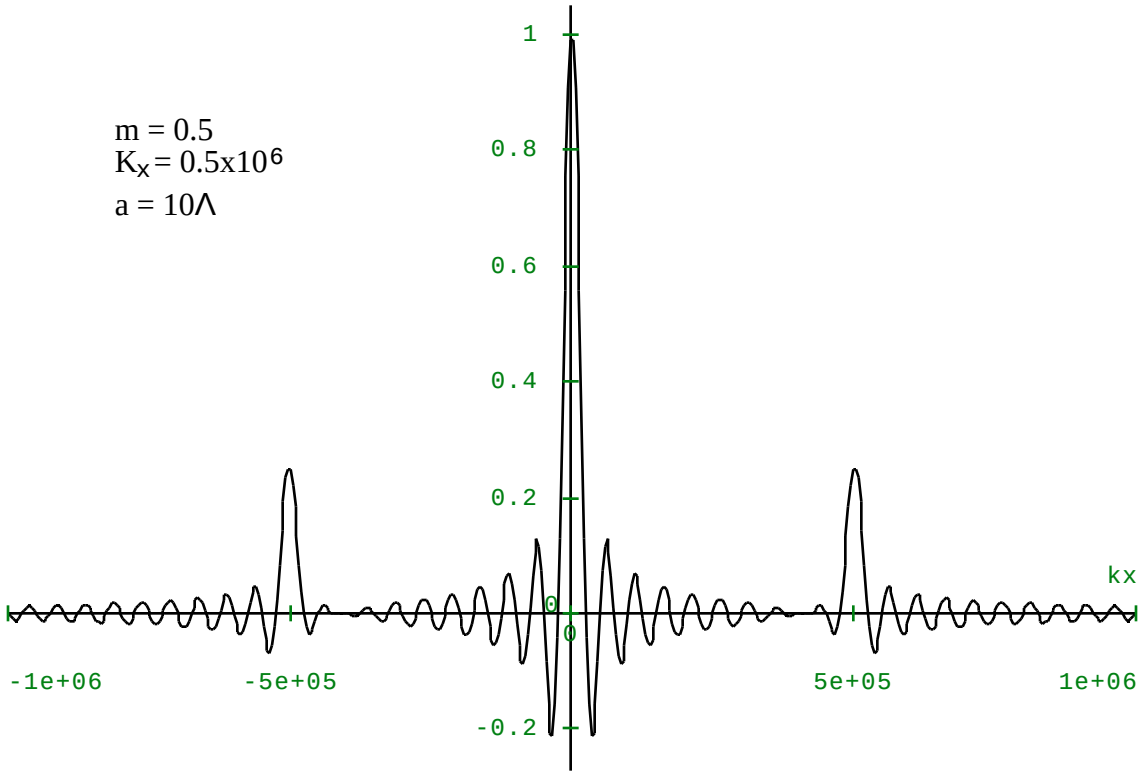

Figure 4. Normalized plane wave spectrum showing sinc functions caused by finite-sized illumination, convolved with shifted delta functions caused by grating

$$I(k_{x'},x_o) \quad E_o^2 \left[\frac{4}{k_{x'}^2} \sin^2(k_{x'}a) + \frac{m^2 \sin^2((K_x+k_{x'})a)}{(K_x+k_{x'})^2} + \frac{m^2 \sin^2((K_x-k_{x'})a)}{(K_x-k_{x'})^2} \right.$$
$$+ \frac{4m \sin(k_{x'}a) \cos(K_x d)}{k_{x'}} \left(\frac{\sin((K_x+k_{x'})a)}{(K_x+k_{x'})} + \frac{\sin((K_x-k_{x'})a)}{(K_x-k_{x'})} \right)$$
$$\left. + \frac{2m^2 \sin((K_x+k_{x'})a) \sin((K_x-k_{x'})a) \cos(2K_x d)}{(K_x+k_{x'})(K_x-k_{x'})} \right] \qquad (13)$$

It should be noted that eqs.(10-12) represent the plane wave spectrum with respect to the variable x'. Equation 13, however, is identical for $k_{x'}$ or k_x. This can be easily explained as follows: E(x') = E(x) * δ(x-d), (where * denotes convolution), and convolution in the spatial domain transforms into a multiplication in the plane wave spectrum. The inverse Fourier transform of a shifted delta function is a complex exponential, and when finding the intensity of

the plane wave spectrum, one multiplies $A(k_x)$ by its complex conjugate, which will result in this complex phase term becoming unity.

III. Numerical Analysis

In order to understand the implications of eq. (13), it is plotted in this section using *Maple V* for various parameter values. Unless stated otherwise, each plot varies the position of the knife edge over the extent of the beam, i.e. $-L/2 < x_o < L/2$, along one graph axis, and uses $\lambda = 0.628$ μm. When the intensity is also shown as a function of k_x (3-d plots), values are plotted from $k_x = 0$ to $2\pi/\lambda$, showing all of the propagating plane waves (the total power in which could be collected with a N.A. = 1 lens). In showing intensities, positive and negative k_x yield identical results, so only positive ones are shown.

A. Effect of knife edge position on plane wave spectra of gratings

The first case we analyze is that of a 1.57 μm period ($\Lambda=2.5\lambda$) sinusoidal grating, with modulation index m=1, illuminated by a 15 μm wide beam. According to eq. (13), the spectrum should consist of the squared Fourier transform of the aperture (sinc^2, where $\text{sinc}(x) = \sin(\pi x)/\pi x$), convolved with delta functions at $k_x = 0$ and $\pm 2\pi/\Lambda$.

Figure 3 depicts this plane wave spectrum. As may be expected, as the knife edge obscures more of the illuminating beam, the spectrum intensity decreases. The important point to note though is that as the knife edge is moved, the entire spectrum carries the spatial details of the grating. This is apparent in figure 3 as the x_o-dependent wavy structure superimposed on the plane wave spectrum, *even at $k_x=0$* along the crests of the plot. This last point is very important, since it implies that *even if a very low numerical aperture system is used to collect the plane waves, the grating information can still be recovered*. The specifics of this recovery will be discussed later.

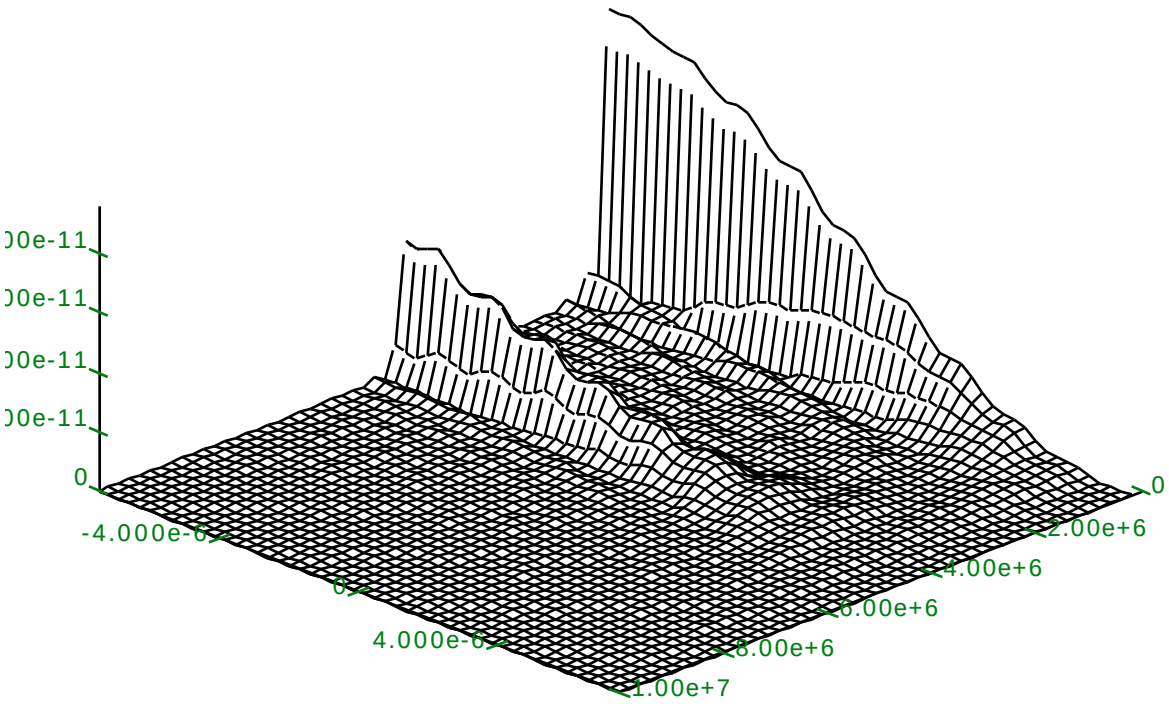

Figure 3. Propagating plane wave spectrum intensity graph of Eq. (13) for 1.57-µ grating

Figure 4 shows a similar plane wave spectrum but for a 0.314 µm period ($\Lambda=\lambda/2$) grating with a modulation index of 1, illuminated by a 3 µm wide beam. Note that although an evanescent wave pattern with amplitude 1/2 exists at $\pm$ $2x10^{-7}$, similar to the half amplitude crest at $4x10^{-6}$ in Fig. 3, it is not shown in this figure which excludes evanescent waves.

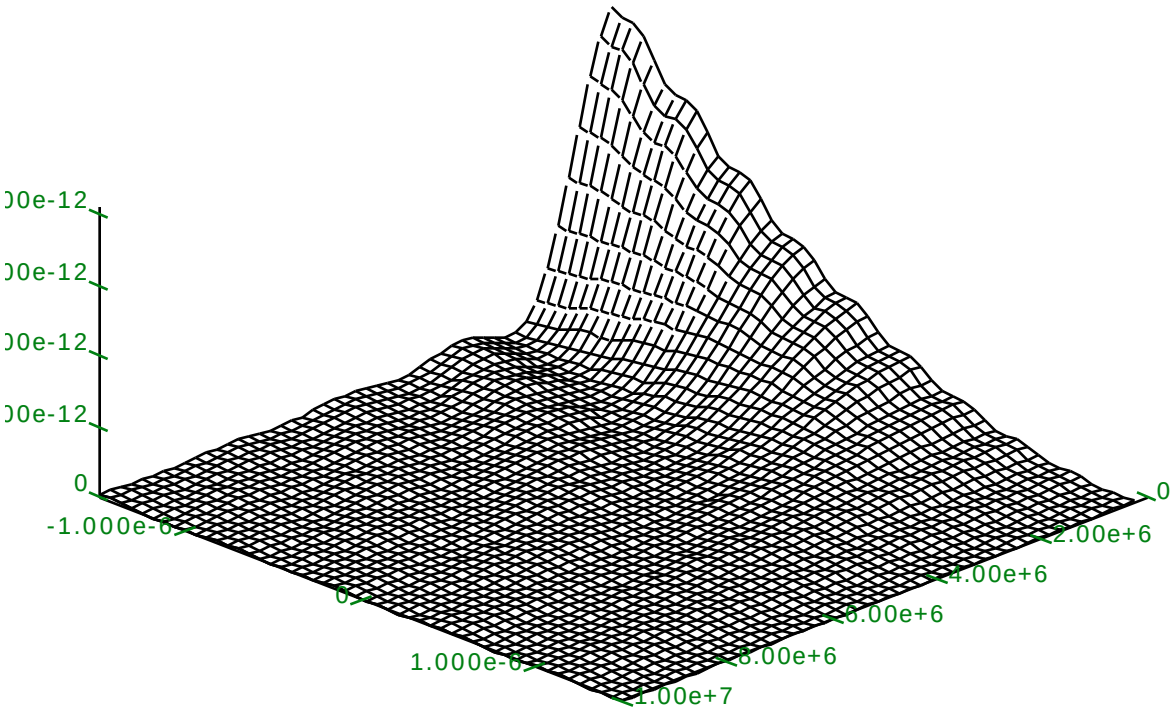

Figure 4. Propagating plane wave spectrum intensity graph of Eq. (13) for 0.314-µm grating

Figure 5 depicts the optical power in the spectrum of figure 4 as a function of x_o. This is defined as the integral of $I(k_x,x_o)$ over $k_x = 0..2\pi/\lambda$ which is equivalent to the total power available for detection with a N.A.= 1 system. Note that there are approximately 10 sinusoidal variations as x_o varies from -1.5 to 1.5 µm, which corresponds to the distance the knife edge moved (L=3 µm), divided by the grating period (Λ=0.314 µm). When the knife edge moves through a section of the grating that is not transmissive (for example at x_o=0.157 µm), the x-dependent optical power is constant (i.e. $dI/dx_o=0$). This is intuitively satisfying since when the edge is at a point where the

grating completely blocks all light, moving the knife edge in either direction should not change the power in the plane waves.

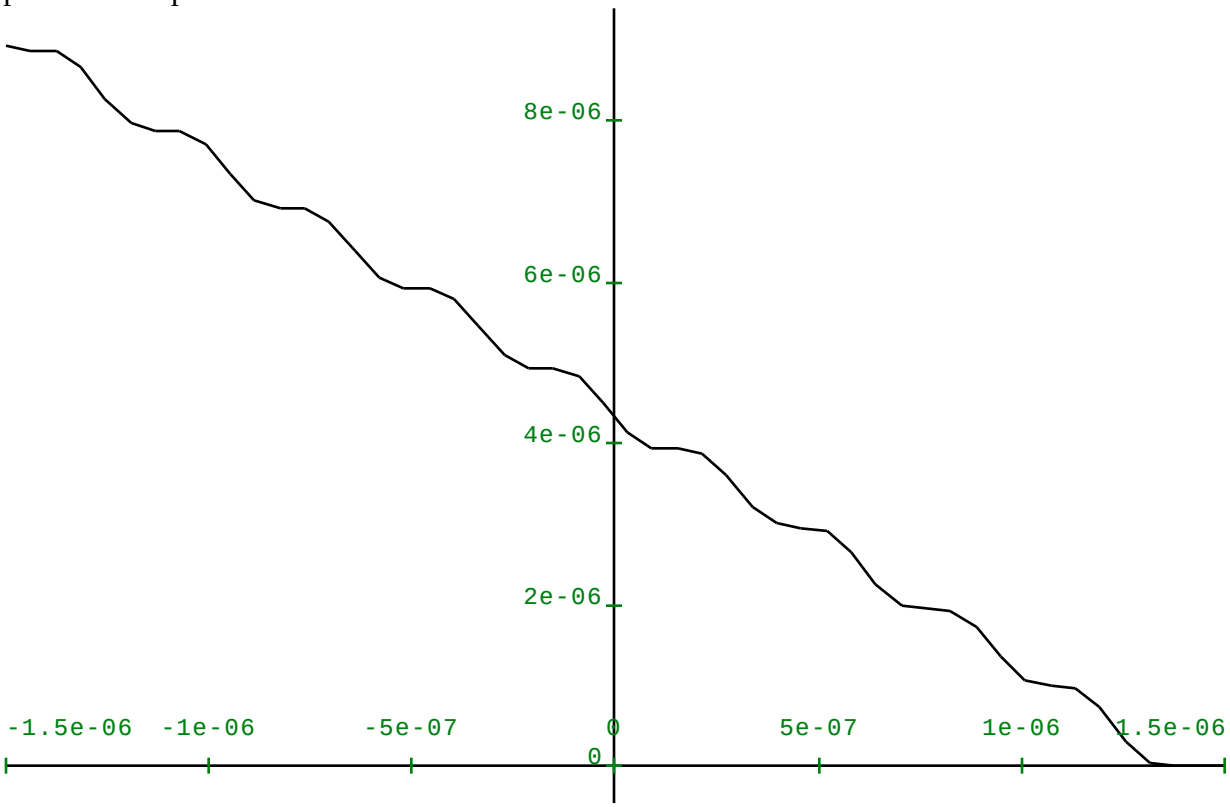

Figure 5. Propagating optical power of plane wave spectrum intensity for 0.314 μm grating

B. Retrieval of object transmittance

In previous papers [1, 2] it was reasoned that for small displacements of the knife edge, the reduction in transmitted light power should be linearly proportional to the knife edge movement. The proportionality constant is dependent on the intensity transmission characteristics of the specimen and the beam power at the knife-edge. Specifically,

$$\frac{dP}{dx_o} \quad |t(x_o)|^2 \tag{15}$$

Equation (15) implies that to retrieve the intensity transmittance of the specimen from the photodetector, one should take the derivative of total power (including evanescent power) with

respect to x_o. Taking d/dx_o of figure 5 (propagating power only) results in figure 6. It is evident from this graph that this reveals the grating structure with much increased contrast. The results for a 0.0314 μm grating (λ/20), with m=1 and L=3 μm are given in figure 7.

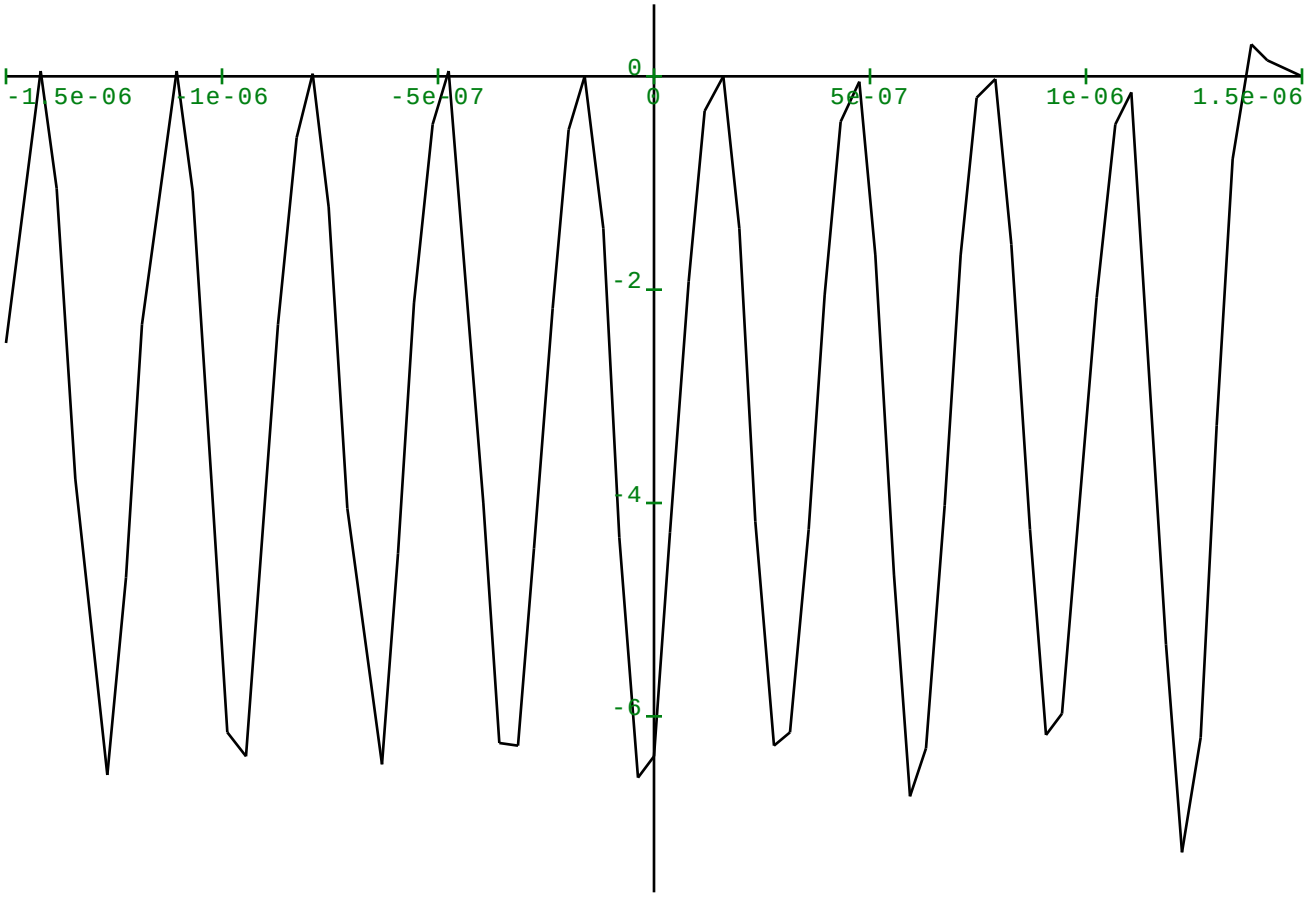

Figure 6. Derivative of 0.314 μm grating propagating power with respect to x_o

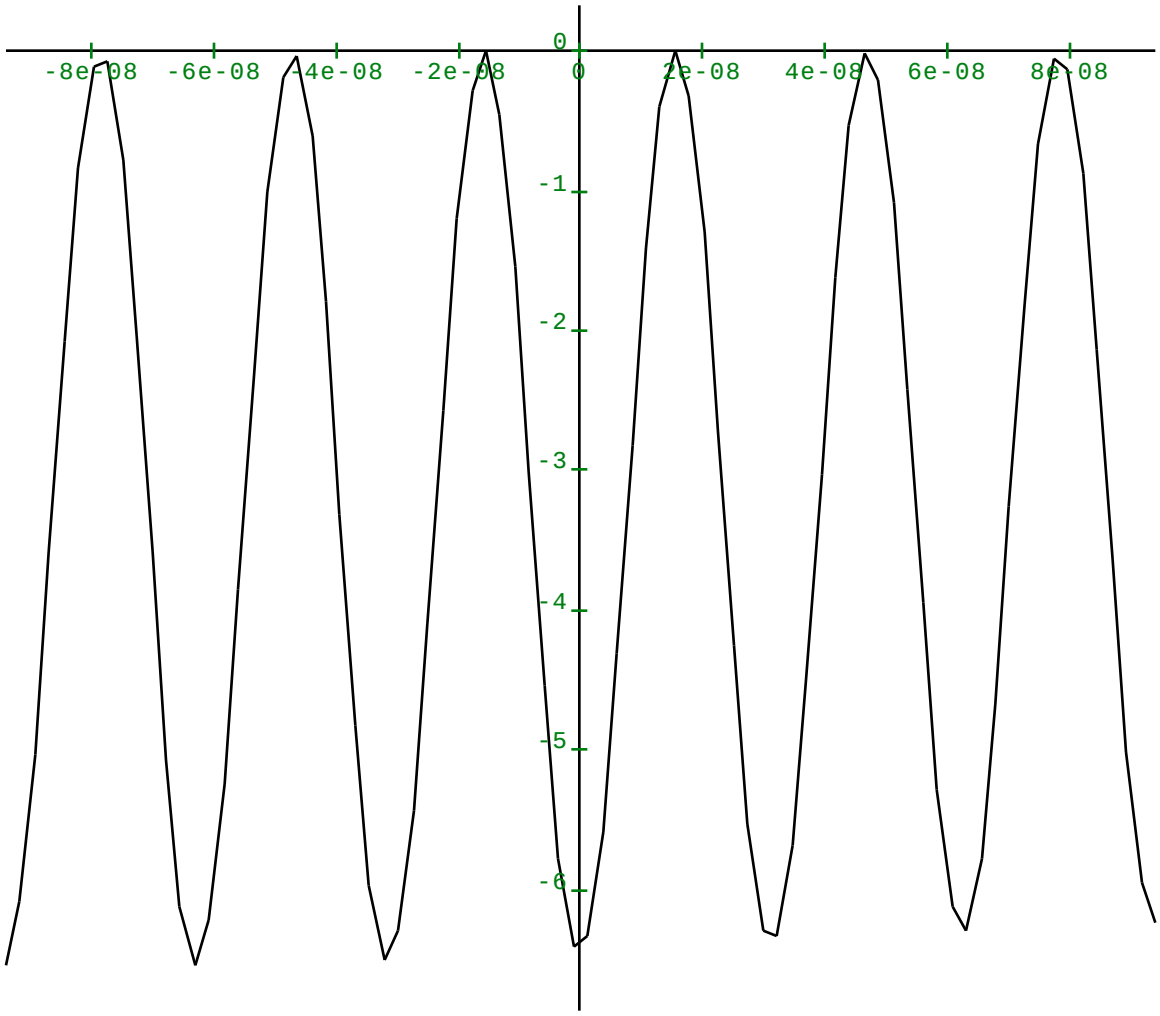

Figure 7. Derivative of 0.0314 μm grating propagating power with respect to x_o

If the knife-edge is vibrated in the x-direction about the point x_o, with peak-to-peak amplitude Δx, the time-modulated power at the photodetector would have a peak-to-peak variation of $\Delta x \cdot dP/dx_o$. This is proportional to the peak-to-peak AC electrical signal at the output of a photodetector. By scanning the entire object under the vibrating knife edge, an image of t(x) may be reconstructed. Scanning the object past the knife-edge would be preferential to moving the knife-edge past the object, since the latter changes the effective beam width, and hence the propagating (detected) optical power.

IV. Comparison of knife edge and physical apertures

It is instructive to compare the operation of the knife edge electronic aperture with the physical slit aperture. For this comparison, the metal (knife edge, physical aperture) is assumed to be infinitely conducting and thin. All of the propagating waves (i.e. all $k_x = -2\pi/\lambda \,..\, 2\pi/\lambda$) created by either aperture are assumed to be collected.

Figure 8 illustrates the propagating power as a function of knife edge position for a constant transmissive object (m=0), illuminated by a 3 μm wide beam. The total detected power decreases linearly as x_o increases (i.e. the slit width decreases) for most of the plot. This is what one might expect, since as the effective beam (slit) width decreases, more of the beam is geometrically obscured, and thus less light is available in the plane wave spectrum. For large slit widths, the lost evanescent power created by the slit is negligible compared to the propagating power. As the slit becomes very narrow ($<\lambda/2$), this is no longer the case because the narrow slit starts generating significant evanescent waves. The total detected power now decreases quadratically with the slit width, as illustrated in figure 9 (blowup of figure 8 near the point $x_o=L/2$). This result should be compared to that found in [5] which states a width^4 dependence on output power for small *2-dimensional* apertures.

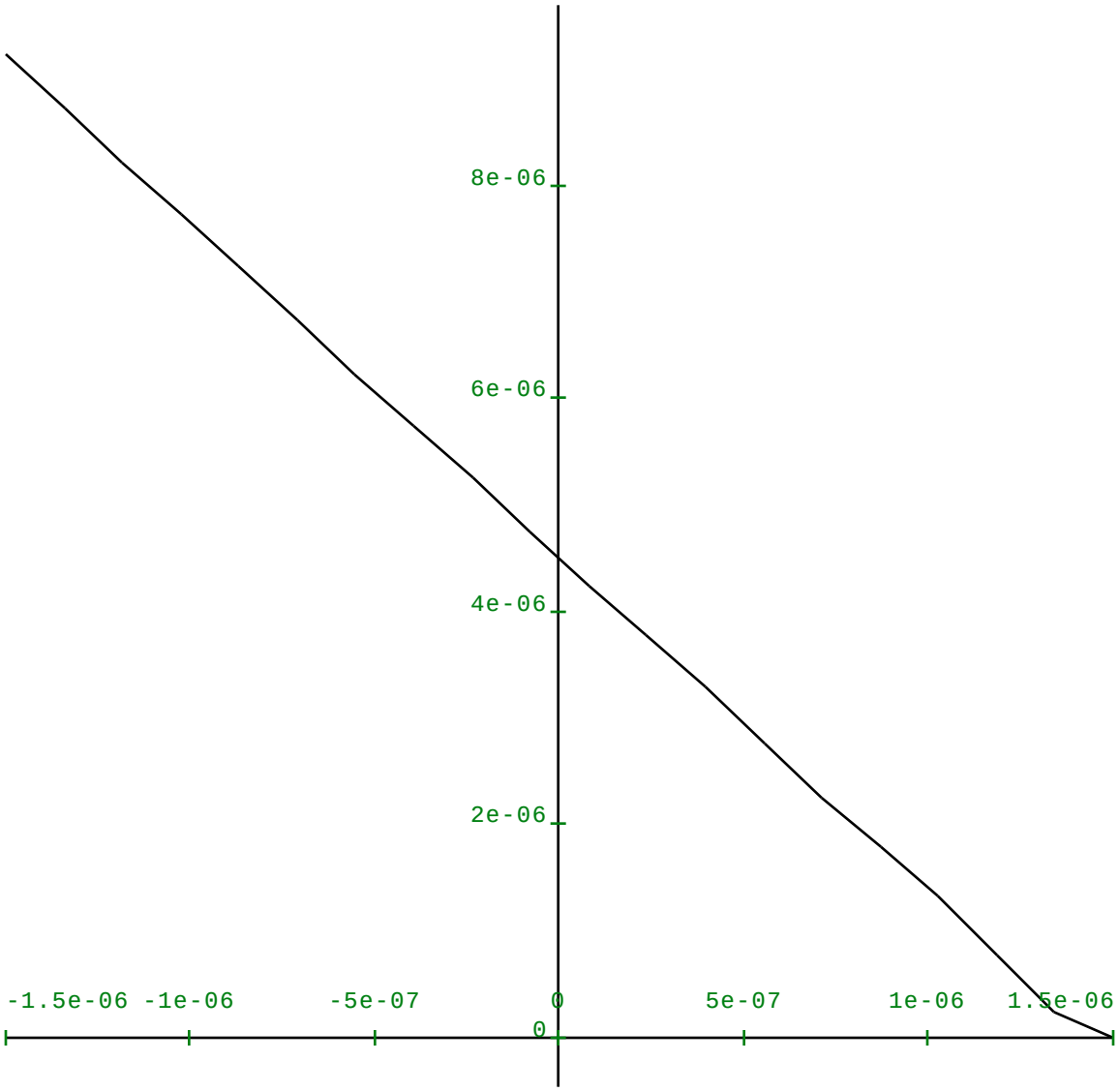

Figure 8. Propagating power for a constant transmissive object

As previously stated, multiplying the x-derivative by Δx yields the peak-to-peak power variation detectable at a photodetector, i.e. the peak-to-peak signal is $dP(x_o)/dx_o \cdot \Delta x$. As an example, choosing $x_o=0$, and $\Delta x=1$ μm would give an output of approximately $3.2 \cdot 1x10^{-6} = 3.2x10^{-6}$, where $dP(0)/dx_o$ is numerically determined from figure 8 at $x_o=0$. This is the same signal as would be achieved with a 1 μm wide physical aperture (figure 8-marked with a '+') and

the entire incident light modulated by a "sinusoidal" chopper. Thus, for large sampling apertures, the vibrating knife edge sampler offers no signal improvement over the physical aperture sampler.

However, for small ($<\lambda/2$) apertures, the knife edge aperture appears to offer a significant improvement in received signal. This may be seen by looking at, for example, a 0.05 μm wide aperture. The physical slit's propagating power is ~2.5×10^{-8} ('+' in figure 9). For the knife edge created aperture at $x_0=0$, the detectable signal is $3.2 \times 0.05 \times 10^{-6} = 1.6 \times 10^{-7}$, or *6.4 times larger* than the physical slit's. Decreasing the aperture size further increases the advantage of using a knife-edge aperture over a physical aperture. This advantage arises from the fact that the small knife edge-created aperture is able to utilize much more of the information originating from the sampling point, whereas the physical aperture causes most of the information to be converted and lost as evanescent waves.

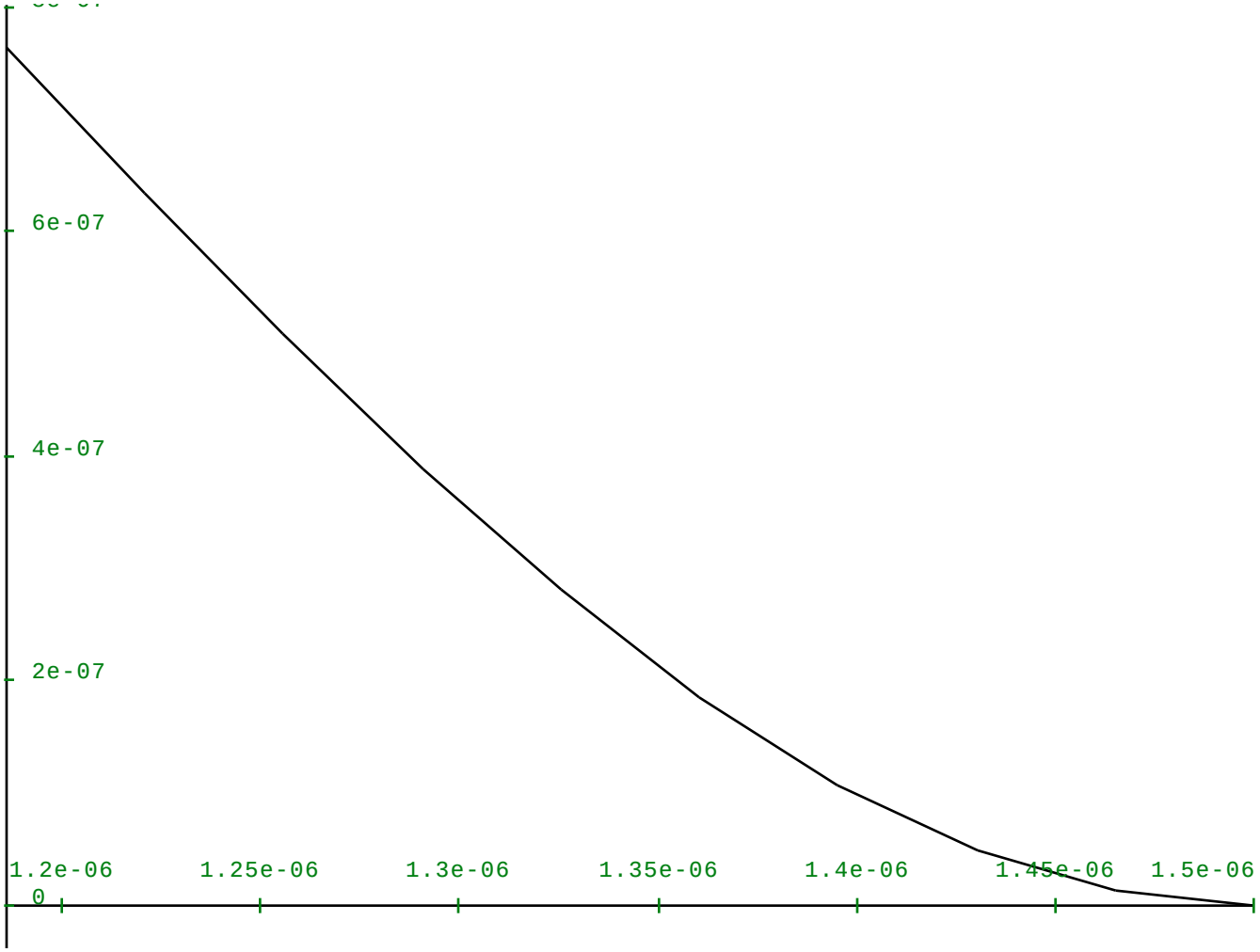

Figure 9. Propagating power for a constant transmissive object (sub-wavelength aperture)

Mathematically, the advantage of the slit aperture may be shown as follows. Consider a one-dimensional slit with width 2a. The slit is illuminated by plane waves with amplitude E_o. The plane wave spectrum of the passed light is readily calculated as $E_o \cdot 2a \cdot \text{sinc}(k_x \cdot a/\pi)$. Again, we assume that plane waves with wavenumber less than $2\pi/\lambda$ are detectable. The optical power is calculated as

$$P = E_o^2\,(2a)^2 \cdot \frac{1}{2\pi} \int_{-2\pi/\lambda}^{2\pi/\lambda} \mathrm{sinc}^2(k_x \cdot a/\pi)\, dk_x \qquad (16)$$

For $2a << \lambda$, i.e. for very narrow slit widths, eq. 16 becomes approximately

$$P \sim E_o^2 \cdot (2a)^2 \cdot 2/\lambda \qquad (17)$$

and for $2a >> \lambda$, eq. 16 becomes approximately

$$P \sim E_o^2\,(2a)^2\,\frac{1}{2a} = E_o^2 \cdot 2a \qquad (18)$$

One-dimensional NSOMs, having narrow *physical* apertures, will yield a signal given by eq. 17. We previously found that to retrieve the object information with the *vibrating knife edge*, one needs to take the spatial derivative of the optical power, multiplied by the peak-to-peak vibration extent (Δx). It is assumed that the illumination extent is larger than λ, i.e. eq. 18 holds. The ratio of the signal found from the two methods is therefore

$$\frac{\mathrm{Signal}_{\text{vibrating knife edge}}}{\mathrm{Signal}_{\text{physical aperture}}}_{1\text{-D}} = \frac{E_o^2\,\Delta x}{E_o^2 \cdot (\Delta x)^2 \cdot 2/\lambda} = \frac{\lambda}{2\Delta x} \qquad (19)$$

where for comparison of similar sized samplers, $2a = \Delta x$ for the physical aperture.

As an example, for the case of 0.05 μm samplers, with $\lambda = 0.628$ μm, the improvement in signal from the vibrating knife edge sampler over the physical aperture is $(0.628 / 2 \cdot 0.05) = 6.28$. This may be compared to the value 6.4 found from the Maple plots.

V. Conclusion

In this paper, it was shown that a vibrating knife edge can be used to sample optical fields, even if they contain sub-wavelength spatial information. In addition, this type of field sampler was found to be more efficient as regards signals received, than the physical apertures such as pipettes used by others [5-7] for small sampling apertures, with the advantage becoming more

pronounced as the aperture size is decreased. However, it should be noted that this does not necessarily imply that the signal to noise ratio is better. To answer that question more should be known about the system (e.g. if it is limited by shot noise, Johnson noise or laser fluctuations). Such an analysis is outside the scope of our paper.

Acknowledgments

This research is supported by the Army Research Office under Grants DAAL-03-91-G-0014 and DAAL-03-92-G-0207.

References

[1] A. Korpel, D.J. Mehrl, and S. Samson, "Beam profiling by vibrating knife-edge: Implications for near-field optical scanning microscopy," Int. J. Imaging Syst. Technol. 2, p. 203-208 (1990).

[2] A. Korpel, S. Samson, and K. Feldbush, "Two-dimensional operation of a scanning optical microscope using a vibrating knife-edge corner," Int. J. Imaging Syst. Technol. 4, p. 207-213 (1992).

[3] S. Samson and A. Korpel, "Two-dimensional operation of a scanning optical microscope by vibrating knife-edge tomography," Applied Optics 34, p. 285-289 (1995).

[4] A. Korpel, S. Samson and K. Feldbush, "Progress in vibrating stylus near-field microscopy," Near Field Optics, ed. D.W. Pohl and D. Courjon, p. 399-406 (Kluwer Academic Publishers, 1993).

[5] G.A. Massey, "Microscopy and Pattern Generation with Scanned Evanescent Waves," Appl. Opt., 23, p. 658-660 (1984).

[6] D.W. Pohl, W. Denk and M. Lanz, "Optical Stethoscopy: Image recording with resolution l/20," Appl. Phys. Lett., 44, p. 651-653 (1984).

[7] E. Betzig, M. Isaacson, H. Barshatzky, A. Lewis and K. Lin, "Super-resolution imaging with near-field scanning optical microscopy (NSOM)," Ultramicroscopy, 25, p. 155-164 (1988).

[8] J. Goodman, Introduction to Fourier Optics, McGraw-Hill Book Co., p. 48-51 (1968).

[9] A. Korpel, H.H. Lin and D.J. Mehrl, "Convenient Operator Formalism for Fourier Optics and Inhomogeneous and Nonlinear Wave Propagation," J. Opt. Soc. Am. A, 6, p. 630-635 (1989).